sustainability

MDPI

Article

Effect of Damage Severity and Flexural Steel Ratio on CFRP Repaired RC Beams

Moatasem M. Fayyadh [1,*] and Hashim Abdul Razak [2]

[1] Asset Lifecycle, Sydney Water, Sydney, NSW 2150, Australia
[2] Department of Civil Engineering, University of Malaya, Kuala Lumpur 50603, Malaysia
* Correspondence: moatasem.m.f@gmail.com; Tel.: +61-4-4907-7730

Abstract: The study aims to investigate the effectiveness and failure modes of using CFRP-bonded sheets as a flexural repair system for RC beams, considering the effect of pre-repair damage levels and flexural steel design limits. This study investigated two different flexural design criteria: RC beams reinforced with the minimum flexural steel limit (ρmin) and RC beams reinforced with the maximum flexural steel limit (ρmax). Additionally, three pre-repair damage levels were considered: design limit load, steel yield limit load, and failure limit load. The study results showed that the RC beams' repair effectiveness depends on the ratio of the flexural steel provided. Specifically, the beams with a minimum steel ratio demonstrated a higher capacity restoration of 49% to 85% (corresponding to the pre-repair damage level, i.e., design load to failure load), while beams with a maximum steel ratio only achieved a capacity restoration of 15.3% to 28.4%. Regarding failure modes, the beams experienced an intermediate-induced crack (IC) debonding due to pre-repair flexural cracks. Despite the debonding of the CFRP sheets, the beams still had the ability to withstand loads close to their unrepaired capacity. This indicates the possibility of re-repairing the beams after the CFRP debonding. Overall, the findings of this study can be used in the industry to repair RC beams and girders that have been damaged due to extreme loading conditions or other reasons. By using CFRP externally bonded sheets, the capacity of the structures can be restored regardless of the pre-repair damage level and the flexural steel design criteria.

Keywords: CFRP sheets; CFRP—concrete bond; design steel ratio; flexural capacity; debonding failure and failure modes

Citation: Fayyadh, M.M.; Abdul Razak, H. Effect of Damage Severity and Flexural Steel Ratio on CFRP Repaired RC Beams. *Sustainability* **2023**, *15*, 7728. https://doi.org/10.3390/su15097728

Academic Editor: José Ignacio Alvarez

Received: 13 March 2023
Revised: 2 May 2023
Accepted: 3 May 2023
Published: 8 May 2023

1. Introduction

In the 1960s, research into the use of FRP first started in Europe [1]. In 1984, the Swiss Federal Laboratory for Materials Testing and Research conducted the first study on the use of FRP plate bonding [2]. The use of FRP materials can be advantageous because of their high tensile strength as well as their outstanding corrosion resistance, fatigue resistance, good performance at increased temperatures, low density, and high specific stiffness and strength [3]. In recent years, there has been a significant increase in growth thanks to a rise in the demand for structural performance improvement and retrofitting activities all over the world. It was discovered that increasing the ultimate capacity of concrete beams by strengthening them with FRP plates that were externally bonded increased the capacity by 70% and decreased the size and density of fractures throughout the length of the beam [4–10]. The amount of CFRP used determines how much of an increase in ultimate capacity the concrete beams experience [11,12]. If there is monolithic action between the strengthened beam and the FRP plates, the load capacity of the strengthened beams might potentially rise. This monolithic action could be achieved using a chemical bonding agent, epoxy glue, or mechanical shear connections [13]. It was decided to use CFRP sheets in the retrofitting of a bridge that had been subjected to overload. At the ultimate limit condition, a much more significant rise in the bending stiffness was seen, whereas, at

the service load levels, a relatively smaller increase was observed [14]. When corroded RC beams were repaired using bonded CFRP sheets, the undamaged state stiffness was restored, and the final deflection was decreased compared to the beams that had not been strengthened [15]. The capacity of the reinforced RC beam may be increased by up to 10% to 24% by using CFRP sheets with U-shape anchors [16]. This increase in capacity is dependent on the number of U-shapes that are secured along the beam length. The change in environmental conditions did not impact CFRP plates due to greater quality control throughout the production process; however, the higher temperature affected hand-laid-up CFRP fabric [17]. This was because hand-laid-up CFRP fabric was affected by the change in temperature.

The change in flexural stiffness is a valuable metric that can be used to measure the efficiency of the CFRP repair, and the CFRP repair method may enhance the flexural load capacity of RC beams by up to 83% [18]. The pre-repair damage level significantly impacts the efficacy of the CFRP repair; if the pre-repair damage level is higher, the CFRP repair effectiveness will be poorer, and the steel strain, CFRP strain, and deflection will all be higher after the repair [19]. Regardless of the severity of the cracking that existed before the repair stage, the CFRP strengthening system significantly improved flexural capacity [20]. When strengthening simply supported RC beams with CFRP strips, the CFRP strip does not need to reach farther than half the span length; therefore, lateral anchorages are unnecessary [21]. The CFRP debonding is delayed to some degree thanks to the end anchorages that are a part of the CFRP repair system [22]. Externally bonded CFRP and steel plates are both adequate for repair solutions; however, the performance of CFRP plates is superior [23]. The CFRP strengthening system's effectiveness in increasing structures' safety is not dependent on the size of the CFRP plate [24]. Even though dynamic characteristics are helpful for evaluating CFRP-repaired concrete girders, their accuracy is restricted. This is because dynamic parameters are impacted by the increase of tension and compression pressures at the adhesive layer between the CFRP plates, and the surface of the girder is a result of the repair process [25]. When using the existing ACI models to predict the flexural capacity of a CFRP-repaired beam and comparing the results to experimental data, there is a possibility that there will be a discrepancy of up to 64% [26].

Several different failure mechanisms have been found based on early investigations conducted over the course of the previous decade on the use of bonded FRP plates to beam soffit as a flexural system. These failure modes can be categorised in a general sense as follows: (1) flexural failure by FRP rapture; (2) flexural failure by crushing of concrete at compression; (3) shear failure; (4) concrete cover separation; (5) plate end interfacial debonding; (6) intermediate flexural crack induced interfacial debonding; and (7) intermediate flexural shear crack induced interfacial debonding [27]. Failure modes such as plate peeling, plate debonding, or local failure in the concrete layer between the FRP plate and longitudinal reinforcements can be caused by shear and stress concentration at the cut-off point of the FRP plate, as well as by flexural cracks [3,6,7,11,28–30]. Other possible causes of failure include flexural fractures. The use of the anchoring system mitigates the effects of impact loading, which causes strengthened beams with CFRP plates to fail due to CFRP debonding [31]. This type of failure may be avoided by employing the anchorage system. The tearing of the concrete, the premature shear failure, and the hybrid mode as a mix of modes 1 and 2 were the three brittle failure modes detected for beams reinforced with externally bonded CFRP sheets [5]. It was discovered that the externally bonded FRP plate that was used for reinforcing the concrete beam failed as a concrete cover failure with plate detachment at the site of the applied load inside the shear span of the beam, and this failure proceeded towards the plate end as the plate thickness increased [32]. It is possible for the pretensioning of CFRP rods that are employed to reinforce RC beams to cause the CFRP to rupture and fail [33]. The failure mechanism was changed from CFRP debonding to CFRP rupture [15,16] when a U-shaped CFRP anchor was used as part of the CFRP repair system for corroded RC structures. The reinforced carbon fibre reinforced plastic (CFRP) beam with an externally bonded carbon fibre-reinforced plastic (CFRP) plate broke

due to intermediate crack debonding while employing the glass fibre reinforced plastic (GFRP) fabric, which ultimately caused the beam to collapse due to GFRP rupture [17]. Failure modes are determined by the condition of the pre-repair damage and the fracture pattern; pre-repair cracks lead to an intermediate crack-induced failure mode [18,19]. When employing the FRP system, it is possible to produce significant improvements in stiffness as well as increases in ultimate capacity and failure modes [34]. When CFRP was utilised for shear repair and attached to the beam from the outside, it did not only significantly enhance the ultimate capacity of RC beams but also significantly reduced the beam's deflection [35]. Shear damage may be repaired effectively with CFRP regardless of the extent of the damage, its location, or the presence or absence of shear stirrups [36]. In a study conducted by Hawileh et. al. [37], the impact of externally bonding CFRP sheets to the soffit of shear-deficient RC beams was examined. The results showed an improvement in the concrete shear capacity of the reinforced specimens. Additionally, the study revealed that the flexural longitudinal reinforcement ratio played a significant role in enhancing the shear strength of RC beams. In a study by Elkhabeery et. al. [38], the effectiveness of using CFRP to strengthen and repair steel beams in flexure was investigated. The findings showed that CFRP sheets were successful in reinforcing compact mono-symmetric sections, while their impact on non-compact sections was limited. The study also emphasized the importance of ensuring sufficient bond length to achieve ultimate strength.

Previous research demonstrated that in recent years, there had been an increase in the demand worldwide for structural performance enhancement and retrofitting works that make use of FRP sheets as an externally bonded system. It was discovered that using the prefabricated FRP plate could provide the maximum degree of material consistency and quality control possible. The amount of damage that existed before the repair and the ratio of flexural steel reinforcement affected how well the FRP-bonded sheets were repaired. Although a significant number of scholars have explored the efficacy of FRP bonded sheets as flexural strengthening systems as well as the failure mechanisms of these sheets, a minimal number of researchers have investigated the repair instances, and even fewer have considered the influence of both the pre-repair damage level and the flexural steel ratio. The purpose of this study is to evaluate the efficacy of employing CFRP-bonded sheets for the flexural repair of RC beams as well as the failure modes of doing so, taking into consideration the influence of various pre-repair damage levels as well as the effect of the flexural steel code design restrictions.

2. Experimental Works

In order to investigate the effectiveness of using CFRP sheets for the repair of flexural damaged RC beams with different pre-damage levels and design criteria, six RC beams are prepared for the tests. The clear span length for each beam is 2.2 m, with a beam cross-section of 150 mm and a width of 250 mm. For the flexural structural design, ACI 318 [39] were used. Based on the ACI Code, there is provision for two limits of the steel ratio in the tension layer as reinforcement requirements for structural elements are subjected to flexure. The minimum steel limit (ρmin) is provided to prevent cracking due to thermal expansion.

In contrast, the maximum steel limit (ρmax) is provided to prevent brittle failure due to concrete crushing. Thus, in this study, considering the two steel ratio limits, one RC beam was designed with ρmin and the other with ρmax, and both steel ratios were used to ensure that the failure is due to steel yielding and not a brittle failure by concrete crushing. For flexural cases, the RC beam bending capacity is calculated using the following Equations from ACI 318 [39].

$$\mathrm{M} = A_s \times f_y \times (\mathrm{d} - \mathrm{a}/2) \tag{1}$$

$$a = \frac{A_s \times f_y}{0.85 \times f'_c \times b} \tag{2}$$

where M is the ultimate bending capacity, A_s is the cross-section area of the flexural reinforcement, d is the effective beam depth, and f'_c is the concrete compressive strength, and b is the beam width.

The RC beams were designed to resist a concentrated load located at the mid-span in addition to the beam self-weight. The flexural beams were designed in shear to ensure that the beam will not fail in shear failure mode, using shear stirrups with close spacing to ensure high shear resistance. The procedure for the flexural design using both ρmin and ρmax and the shear design to achieve the highest shear resistance was according to ACI 318 [39] equations. The maximum allowable steel ratio to prevent brittle failure of the concrete, i.e., ρmax, is 0.0136, and the provided maximum steel ratio was 0.0131 by using two 16 mm diameter deformed steel bars as the main flexural reinforcement. The minimum allowable steel ratio to prevent shrinkage cracks, i.e., ρmin, is 0.003. The provided minimum steel ratio was 0.006 using two 12 mm diameter deformed steel bars as the main flexural reinforcement. Two 8 mm diameter round steel bars were used as the compression reinforcement for both design cases. For the shear design, 6 mm diameter bars with a spacing of 50 mm were used along the beam length to achieve the highest shear resistance. Figure 1 shows the cross-section detail for both beams, i.e., ρmin and ρmax.

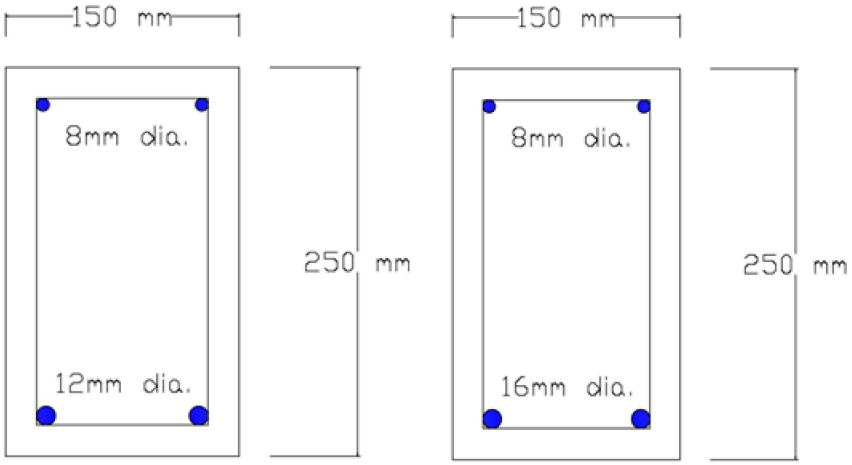

Figure 1. Cross section detail for flexural beams, with ρmin (**left**) and with ρmax (**right**).

The Classification of the RC beams according to damage levels and design case are shown in Table 1. The properties of the concrete and steel bars for the RC beams are shown in Table 2. The round steel bars of 8 mm and 6 mm diameters were tested, and the samples' results were in close agreement with a yield stress of 260 MPa and an elasticity module of 185,000 MPa. After the beam is cast, it is left for one year to avoid any effect of the environment or lifetime on the properties of the materials. It is then tested under point load located at mid-span, where the load is applied gradually at a loading rate of 4 kN/min, i.e., loading and unloading. Figure 2 shows the RC beam under flexural loading conditions.

Table 1. Classification according to Design case and damage level.

Beam No.	Design Case	Load Level
B112m	ρ max	Design limit load
B113m	ρ max	Steel yield limit load
B114m	ρ max	Failure load
B122m	ρ min	Design limit load
B123m	ρ min	Steel yield limit load
B124m	ρ min	Failure load

Table 2. Concrete and steel properties for the RC beams.

Beam No.	Concrete Compressive Strength (MPa)	Concrete Elasticity Modulus (GPa)	Steel Yield Stress (MPa)	Steel Rapture Stress (MPa)	Steel Elasticity Modulus (GPa)
B112m	38	36	480	620	180
B113m	33	29	520	680	180
B114m	30	34	480	620	180
B122m	36	30	535	665	180
B123m	36	33	565	785	180
B124m	35	31	565	785	180

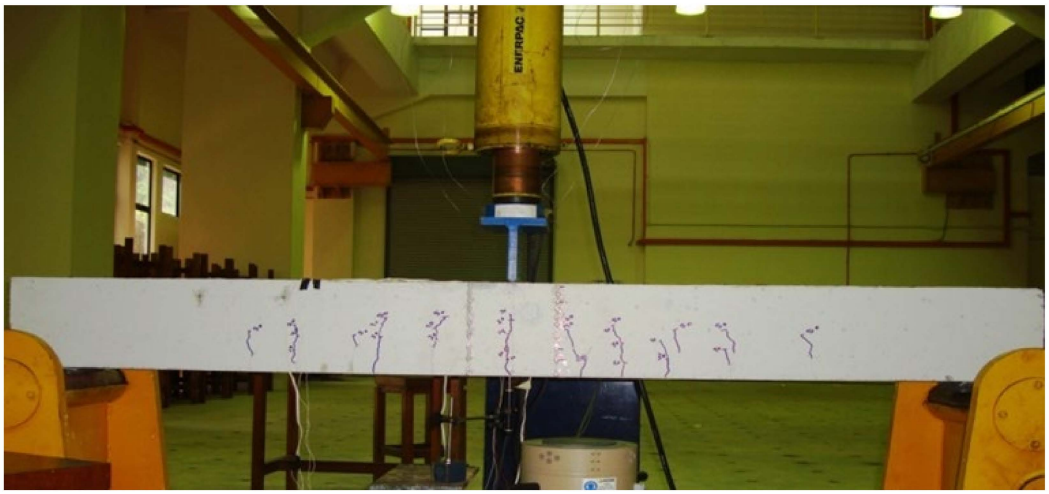

Figure 2. Beam under static test.

For the purpose of repairing, RC beams were turned over, and the tension face was roughened to get a suitable face to give as much friction as possible with the CFRP sheet. Figure 3 shows the roughened surface prepared using a scaling hammer and fixing of the CFRP sheets. The surface was cleaned using an air gun to avoid dust on the surface, as the substrates must be sound, dry, clean, and free from laitance, standing water, grease, oils, old surface treatments or old surface treatments or coatings and all loosely adhering particles. The concrete was cleaned and prepared to achieve a laitance, contaminant-free, open-textured surface. When the concrete surface was prepared, the CFRP sheet was fixed using Sikadur-30 adhesive material and left for one month for hardening. The ACI 420.2R [40] is the design guideline for externally bonded CFRP repairing RC structures. The following assumptions are made in calculating the flexural resistance of the section strengthened with an externally bonded CFRP system, i.e., design calculations are based on the actual dimensions, internal reinforcement arrangement, and material properties of the existing member. The strain in concrete and reinforcement is directly proportional to the distance from the natural axis, which means a plane section before loading remains plane after loading. There is no relative slip between external CFRP and the concrete. The shear deformation within the adhesive layer is very thin, with slight variations in its thickness. The maximum usable compression strain in the concrete is 0.003, and the CFRP has a linear elastic stress-strain relationship to failure.

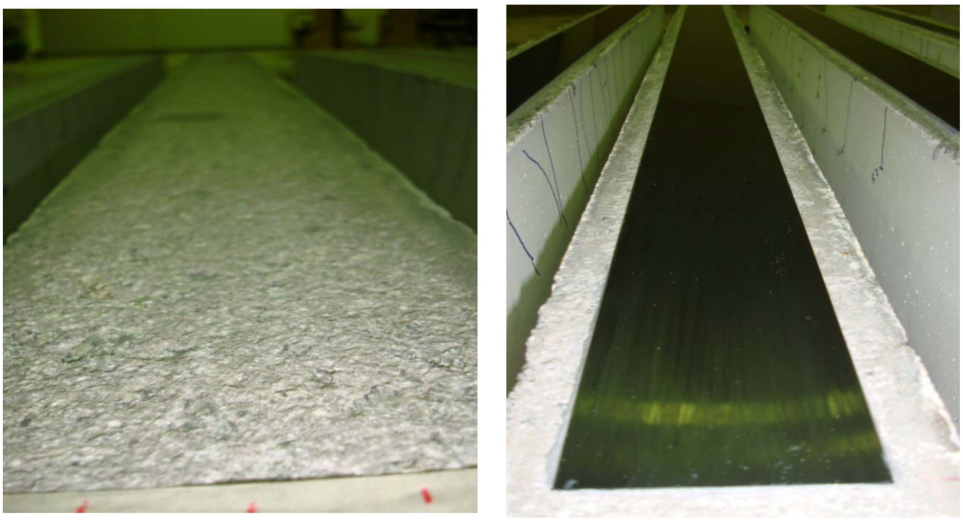

Figure 3. Surface preparation and CFRP fixing.

The ultimate moment capacity of the repaired section according to the ACI 420.2R [40] is shown in Equation (3) as follows:

$$\mathrm{M} = A_s \times f_y \left(\mathrm{d} - \mathrm{B1} \times \mathrm{c}/2\right) + A_f \times f_f \left(\mathrm{h} - \mathrm{B1} \times \mathrm{c}/2\right) \quad (3)$$

where M is the ultimate moment capacity, A_s is the cross-section area of the main steel bars, f_y is the ultimate stress of the main steel bars, d is the effective depth, c is the depth of the neutral axis, A_f is the CFRP cross section area, f_f is the CFRP ultimate stress and h is the beam depth.

$$\mathrm{B1} = 0.85 - 0.008\left(f_c' - 30\right) \quad (4)$$

where f_c' is the concrete compressive strength.

The design of flexural repair with externally bonded CFRP sheets was based on achieving the maximum capacity without debonding failure of CFRP sheets to achieve the highest CFRP strength. The pre-repair damage level was included in the calculation by considering the existing substrate strain value at the tension layer after applying the pre-repair damage load. The existing substrate strain was considered the initial strain and excluded from the strain in the CFRP sheets.

The design procedure was according to the ACI 420.2R [40] equations. For the ρmin group, a CFRP sheet with 100 mm width and 1.2 mm thickness was found to give the highest increase in the capacity before the CFRP debonding. While for the ρmax group, a CFRP sheet with 50 mm width and 1.2 mm thickness gives the highest increase in the capacity before CFRP debonding. The CFRP sheets were designed to be placed on the beam soffit and along the beam length between the supports. According to the manufacturer data sheet, the CFRP material properties are shown in Table 3. The repaired beams were left for 18 days after fixing the externally bonded plate to give the adhesive material sufficient time for its hardening, as suggested by Fayyadh and Abdul Razak [41].

Table 3. CFRP sheet properties.

Properties	Value
Tensile strength (MPa)	2800
Modulus of Elasticity (MPa)	165,000
Ultimate strain (mm/mm)	0.017

3. Results

3.1. Minimum Steel Limit (ρmin)

This section presents the results related to using the CFRP sheet as a flexural repair system when the reinforced beams are designed with the minimum steel limit (ρmin). The effectiveness of the CFRP sheets as a flexure repair system is investigated under the pre-repair damage level, where three damage levels are considered: design load, steel yield load and failure load. The beams with minimum steel are designated as B122m, B123m and B124m. The data from the RC beams' static load test at the pre-and post-repair stages are presented. The static data includes load against deflection curves, load against steel strain curves and load against CFRP strain curves. The crack patterns corresponding to each loading cycle are plotted and appended. This section presents the results for beams B122m, B123m and B124m, designed using ρmin, where two 12 mm diameter steel bars are used in the flexural zone. The beams are then repaired using CFRP sheets according to the repair procedure mentioned in Section 2. The repair is per Code ACI 420.2R [40], and as mentioned in Section 2, a 100 mm width CFRP sheet is used for all the three beams.

Beam B122m is damaged under 25 kN concentrated load at mid-span, which is considered the design limit. After the repair, the load is applied in cycles, where the load cycles and the corresponding number of cracks are shown in Table 4. The load against deflection curves at pre and post-repair stages are shown in Figure 4. The flexural steel strain is monitored by fixing a strain gauge on the steel bars at mid-span, and the data obtained at pre and post-repair stages are shown in Figure 5. For post-repair stages, the CFRP strain is monitored by fixing a strain gauge on the CFRP surface at mid-span, and the data obtained corresponding to each load cycle are shown in Figure 6.

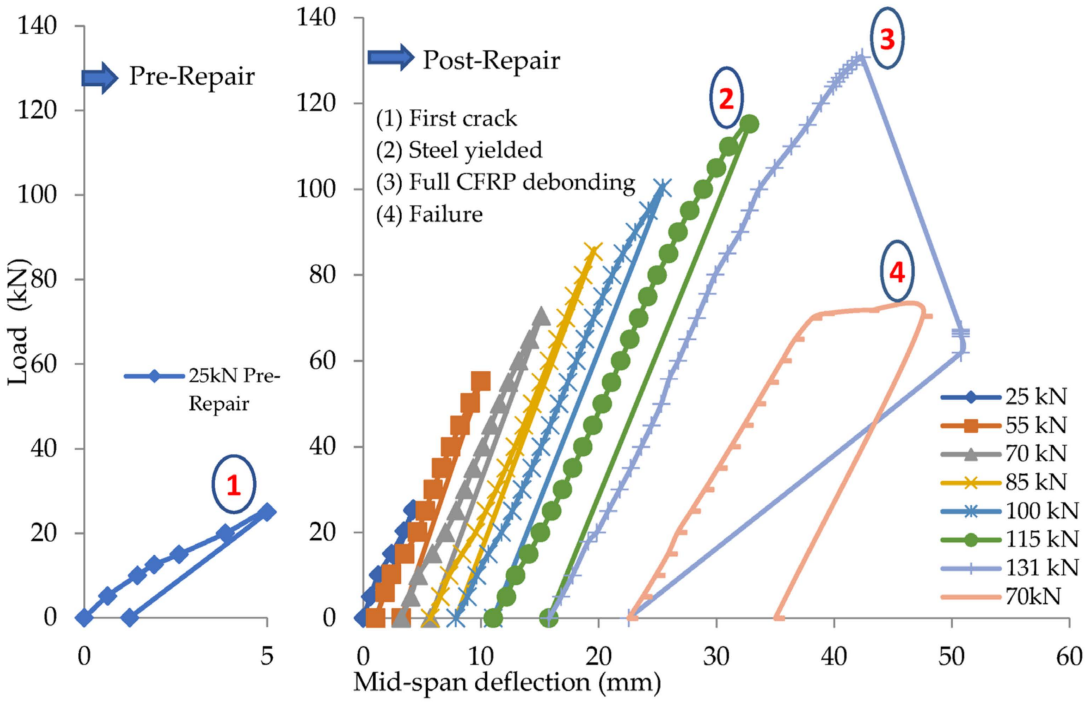

Figure 4. Load against mid-span deflection at pre and post repair stages for beam B122m.

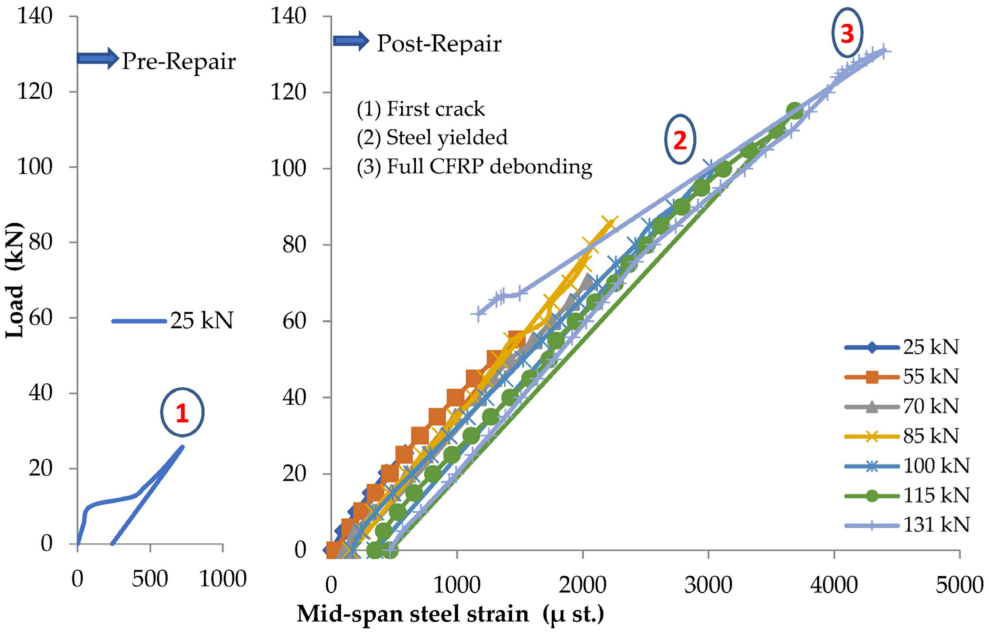

Figure 5. Load against mid-span steel strain at pre and post repair stages for beam B122m.

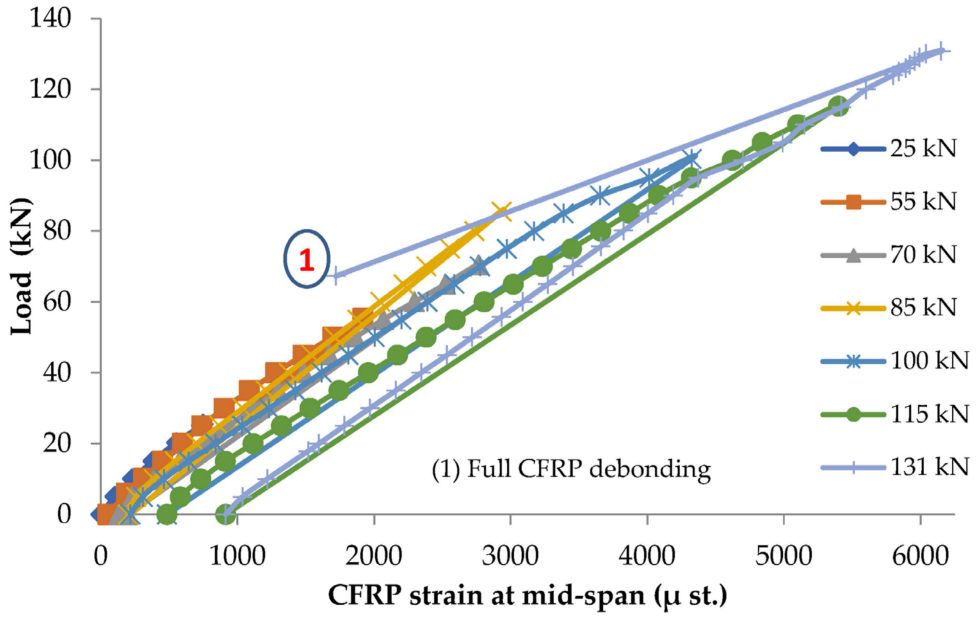

Figure 6. Load against mid-span CFRP strain at post-repair stages for beam B122m.

Table 4. Load cycles and corresponding number of cracks for beam B122m.

Load Cycles (kN)	Number of Cracks	Remark
25	7	Pre-repair stage
25	7	Post-repair stage
55	12	
70	20	
85	21	
100	26	
115	28	Steel Yielded
131	28	CFRP debonded
71	28	Failure

Figures 4–6 show that the repaired beam reaches a load capacity of 131 kN, and the corresponding CFRP debonding strain reaches 6150 µst. Beyond the CFRP debonding point, steel strain shows a rapid decrease corresponding to the rapid decrease in applied load and the rapid increase in deflection as shown in Figure 5. Figure 5 also shows that steel yielded at a load of 115 kN with strain of about 3100 µst. The beam records a steel strain of 4300 µst, less than the rupture strain of steel beyond 6000 µst. This indicates that the steel did not rupture and was the reason behind the ability of the beam to withstand a load of up to 71 kN after the CFRP debonding. This is considered the capacity of the unrepaired section, wherein the CFRP sheets take up most of the tension stresses at the stage before the CFRP debonding. After CFRP debonds, the failure mode is a flexural failure, meaning that the concrete did not fail and the un-ruptured steel takes up all the stresses. The capacity increase due to adding the CFRP sheet is evaluated based on the repaired capacity (131 kN) divided by the unrepaired capacity (71 kN), which gives an increase of 84.5%.

The reinforced beam B123m is damaged under 55 kN concentrated loading at mid-span, which is considered close to the yield limit of the steel reinforcement. After inducing damage, the beam is repaired, and the load is applied in cycles, where the load cycles and the corresponding number of cracks are shown in Table 5. The load against deflection curves at pre- and post-repair stages are shown in Figure 7. The load against steel strain curves at pre- and post-repair stages are shown in Figure 8. For the post-repair stage, the load vs. CFRP strain curves is shown in Figure 9.

Table 5. Load cycles and corresponding number of cracks for beam B123m.

Load Cycles (kN)	Number of Cracks	Remark
55	11	Pre-repair stage
25	11	Post-repair stage
55	16	
70	19	
85	20	
100	24	
115	25	
130	26	Maximum capacity/CFRP start debonding
122	27	CFRP fully debond
80	27	Failure

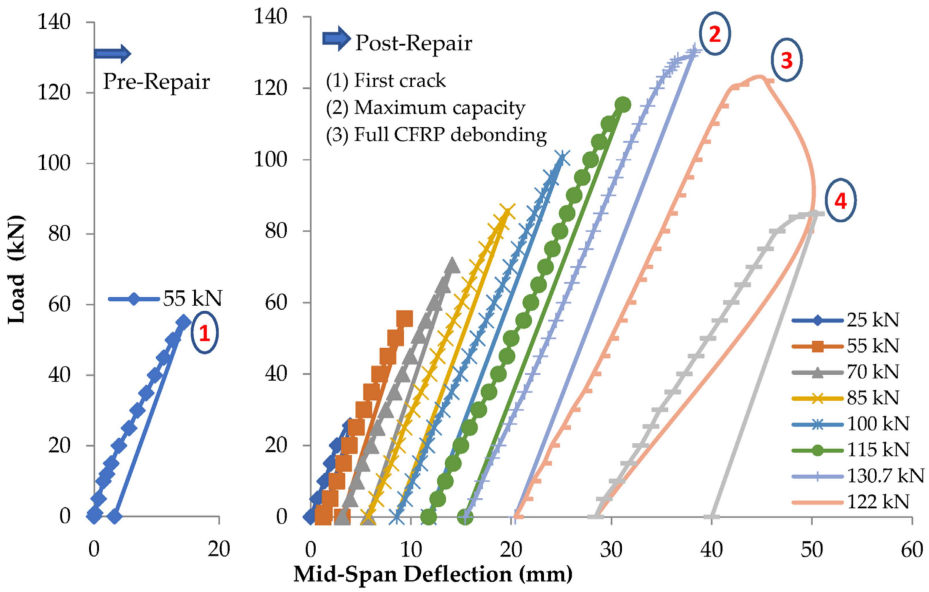

Figure 7. Load against mid-span deflection at pre and post repair stages for beam B123m.

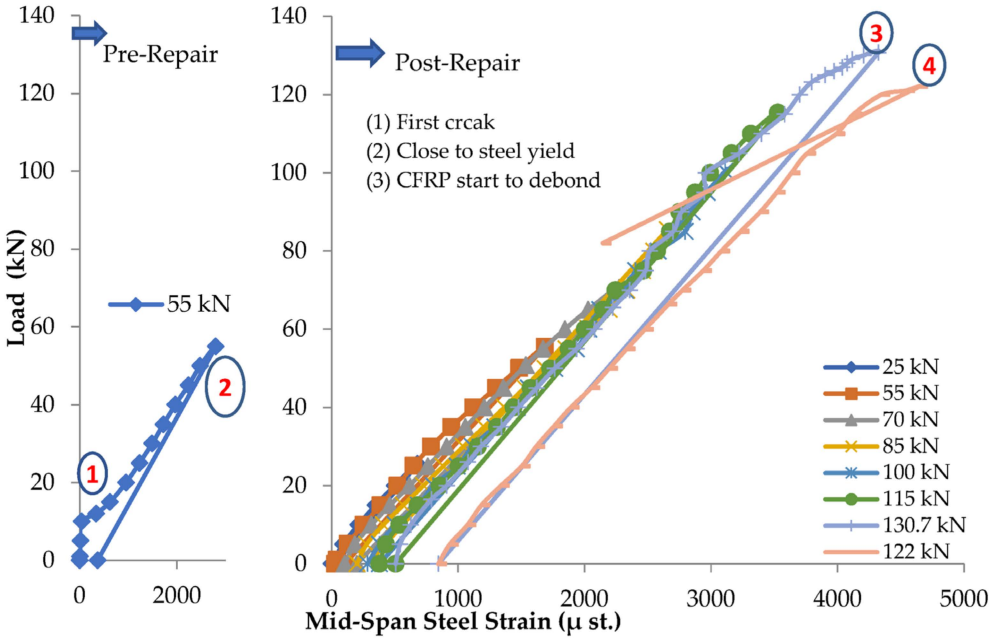

Figure 8. Load against mid-span steel strain at pre and post repair stages for beam B123m.

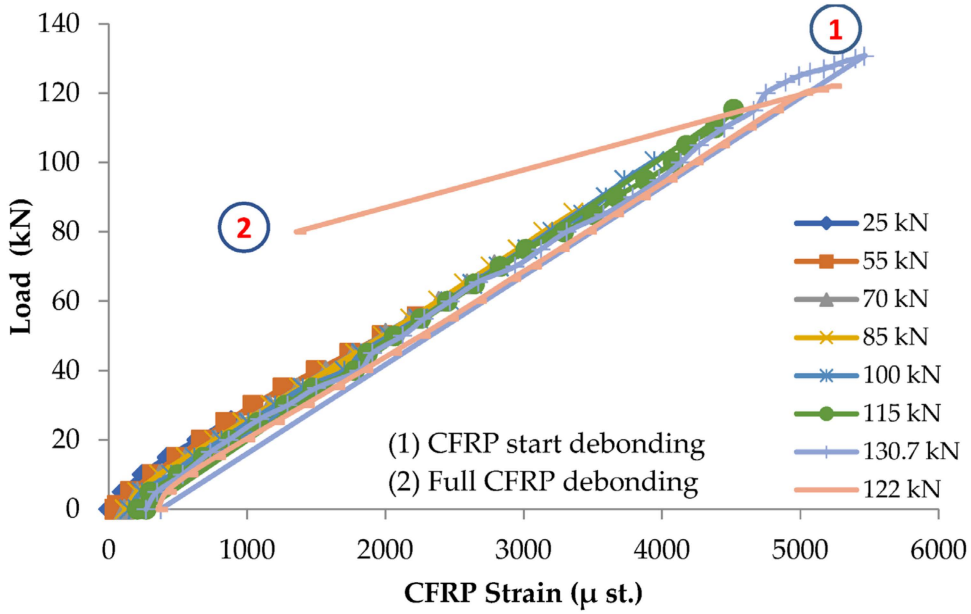

Figure 9. Load against mid-span CFRP strain at post-repair stage for beam B123m.

The results show that the maximum load capacity reached is 130.7 kN, after which the initial debonding begins. Full debonding occurs at 122 kN for the following load cycle, corresponding to a CFRP strain of 5300 μst. Beyond the CFRP full debonding, there is a rapid increase in the deflection corresponding to a rapid decrease in the applied load. Similarly, the steel strain shows a rapid decrease beyond the full debonding of CFRP, corresponding to a rapid decrease in the applied load. The steel reaches a strain of 4700 μst, which is still below the rupture strain. This is the reason behind the ability of the beam to withstand loads of up to 84.8 kN beyond the full debonding of the CFRP sheets, where the failure mode is a flexural failure without concrete crushing. This ability is due to the action of the unruptured steel, which carries all the tension stresses up to rupture beyond 7000 μst, and this load is the capacity of the unrepaired section. The increase in the load capacity by fixing the CFRP sheets, as computed before, is 54.1%.

The reinforced beam B124m is damaged under failure load, which reaches 85.8 kN. The applied load is stopped when the failure is initiated, indicating that the load against the deflection curve becomes horizontal. After the induced damage, the beam is repaired, and the load is applied in cycles. The load cycles and the corresponding number of cracks are shown in Table 6. The load against deflection curves for load cycles at pre and post-repair stages are shown in Figure 10. The load against steel strain curves at the pre-repair stage are shown in Figure 11. No data for the steel strain at the post-repair stage is recorded since the strain gauges were broken when the failure occurred at the pre-repair stage. For post-repair stages, the load against CFRP strain is shown in Figure 12.

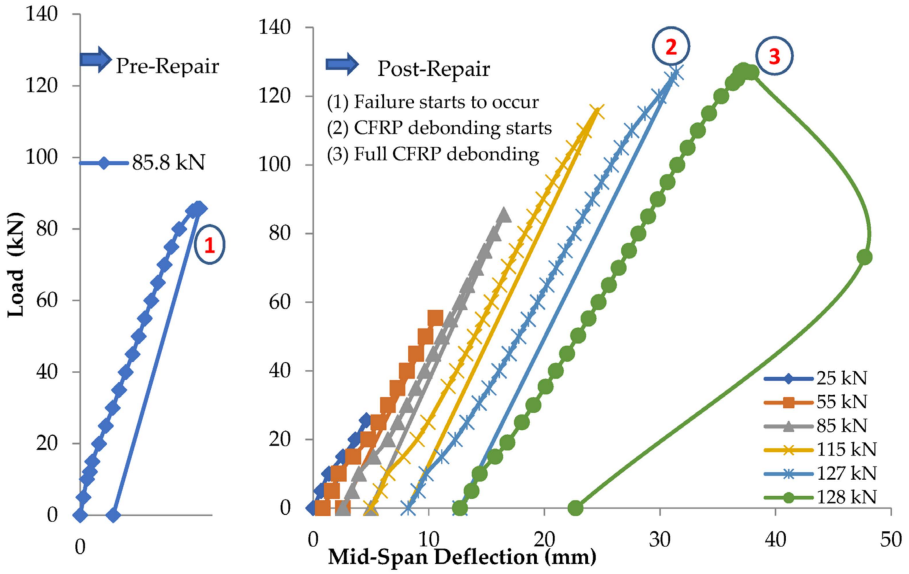

Figure 10. Load against mid-span deflection at pre and post repair stages for beam B124m.

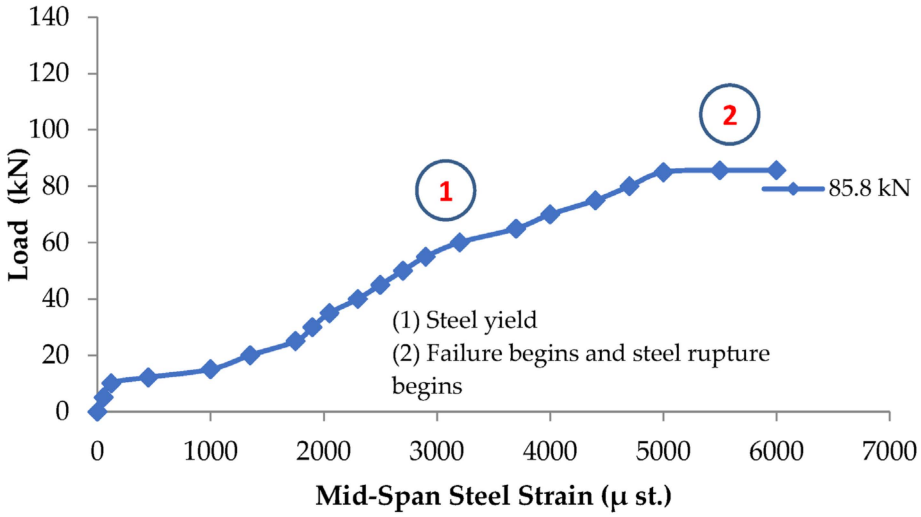

Figure 11. Load against mid-span steel strain at pre-repair stage for beam B124m.

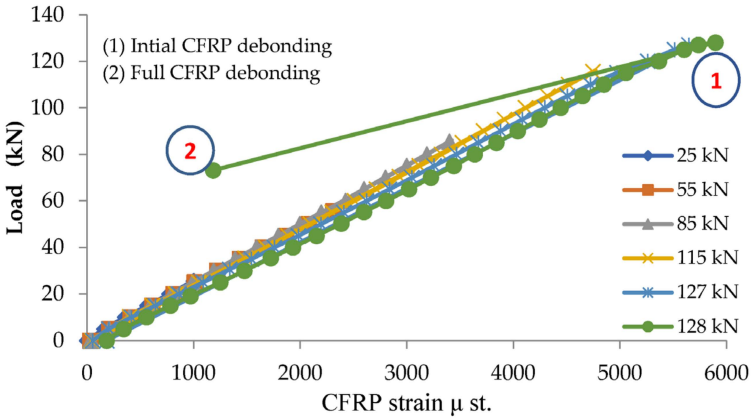

Figure 12. Load against mid-span CFRP strain at post-repair stage for beam B124m.

Table 6. Load cycles and corresponding number of cracks for beam B124m.

Load Cycles (kN)	Number of Cracks	Remark
85.8	15	Pre-repair stage
25	15	Post-repair stage
55	15	
85	16	
115	17	
127.5	19	Maximum capacity/CFRP debonding begins
128	21	CFRP fully debonded

The results show that the failure begins at 85 kN at the pre-repair stage, and the load against the deflection curve becomes horizontal. The steel begins to rupture when it reaches a strain of 6000 μst at 85.6 kN. Following this, the load is released at a load of 85.8 kN, and the strain gauge breaks. The CFRP begins to deboned at 127 kN load, and full CFRP debonding occurs at 128 kN, where the CFRP strain records 5900 μst. When full debonding occurs, there is a rapid increase in the deflection corresponding to the rapid decrease in the applied load. The increase in the load capacity due to the application of the CFRP sheets is 49.2%.

The failure occurs when the flexural cracks at the mid-span extend to the adhesive interface between the CFRP sheets and the concrete surface to induce intermediate cracks, which cause full debonding upon further loading. Figure 13 shows the appearance of intermediate cracks (IC) in the adhesive layer and the full CFRP debonding for beams B122m, B123m and B124m. The failure is governed by the intermediate crack debonding with the CFRP strains between 5400 and 6200 μst. However, the findings by Benjeddou et al. [28] showed that the failure mode for repair work was peeling off CFRP sheets at the ends. The effectiveness of the CFRP repair system at different pre-repair damage levels is highlighted as follows. The damage level is calculated based on the percentage of the applied load at the pre-repair stage to the ultimate capacity of the unrepaired sections. The stiffness recovery, as indicated by the ratio of the increase in the ultimate load capacity, is calculated based on the increase in the ultimate capacity of the repaired sections to the ultimate capacity of the unrepaired sections. Figure 14 shows the repair effectiveness based on the static data of beams B122m, B123m, and B124m, corresponding to 0.35, 0.65 and 1 damage levels, respectively.

Figure 13. Induced intermediate cracks debonding and failure mode for beams B122m, B123m and B124m, from left to right, respectively.

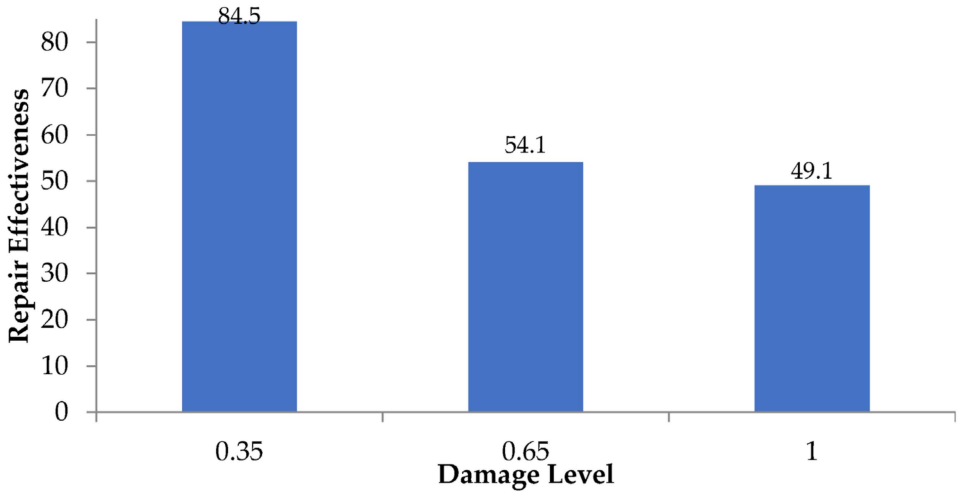

Figure 14. CFRP repair effectiveness based on static data for ρmin group.

The results show that the effectiveness of the repair using CFRP sheets decreases as the pre-repair damage level increases. Regardless, even with the pre-repair damage level at 100%, the repair with CFRP sheets helps to recover the stiffness and increase the load capacity of the repaired beams. At a damage level of 35% which is the design load limit, repair with CFRP sheets increases the ultimate capacity by 85%. At the damage level of 65%, which is close to the steel yield load limit, the increase in the load capacity is reduced, and at a damage level of 100%, the increase in the load capacity is only 49%.

3.2. Maximum Steel Limit (ρmax)

This section covers the results of using CFRP sheets as a flexural repair system when the reinforced steel is designed to be close to ρmax. The effectiveness of the CFRP sheets as a flexural repair system is investigated under the effect of different pre-repair damage levels, where three levels are considered, i.e., design load, close to the steel yield load and failure load. The beams with ρmax are designated as B112m, B113m and B114m. The static data obtained from the static load test of the RC beams at the pre- and post-repair stages are presented. The static data includes load against deflection curves, load against steel strain curves and load against CFRP strain curves. This section presents the results for beams B112m, B113m and B114m, designed using ρmax, where two 16mm diameter steel bars are used in the flexural zone. The beams are then repaired using CFRP sheets according

to the repair procedure mentioned in Section 2. The repair is per ACI 440.2R [40] Code as mentioned in Section 2, where a 50 mm width CFRP sheet is used for all three beams.

Beam B112m is subjected to a damaged load of 40 kN, close to the design load, at the pre-repair stage. After repair, the beam is subjected to load cycles up to failure, as shown in Table 7 presents the load cycles and the corresponding number of cracks. The load against CFRP strain at post-repair stages are shown in Figure 15. The load against deflection curves at pre- and post-repair stages are shown in Figure 16. The load against steel strain curves at pre and post-repair stages are shown in Figure 17.

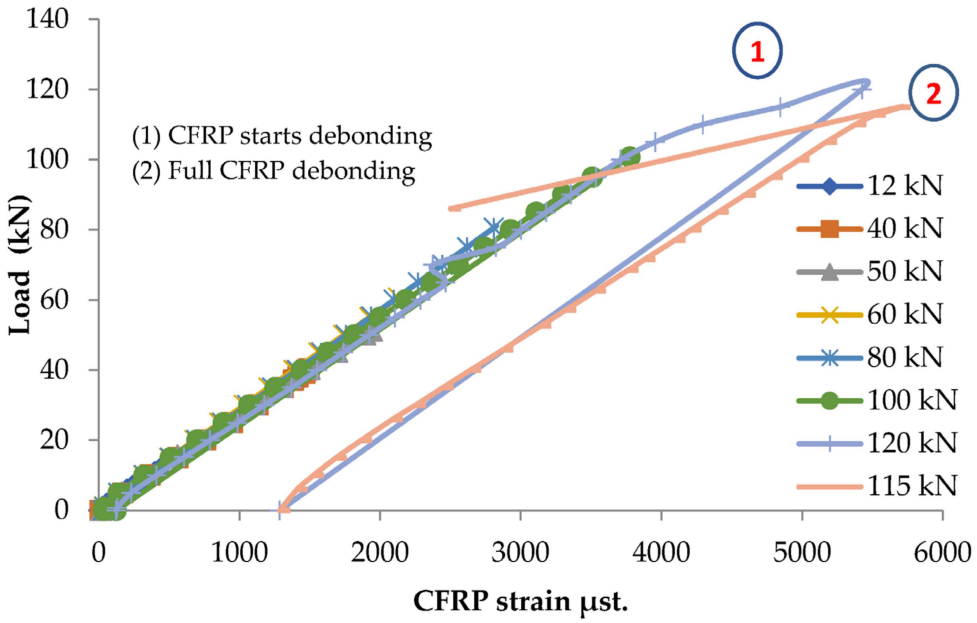

Figure 15. Load against mid-span CFRP strain curves at post-repair stage for beam B112m.

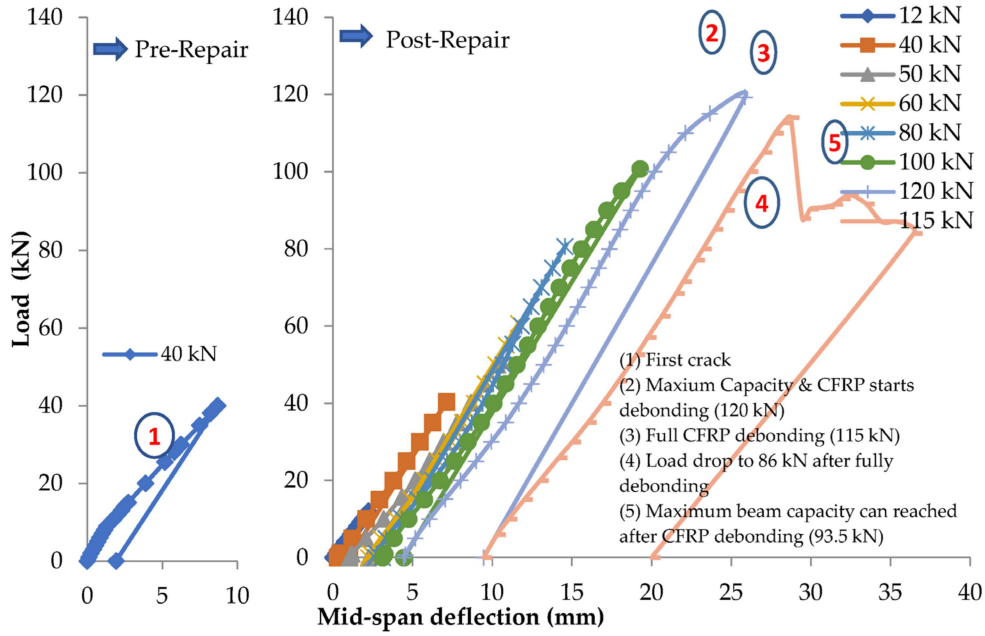

Figure 16. Load against mid-span deflection curves at pre and post repair stages for beam B112m.

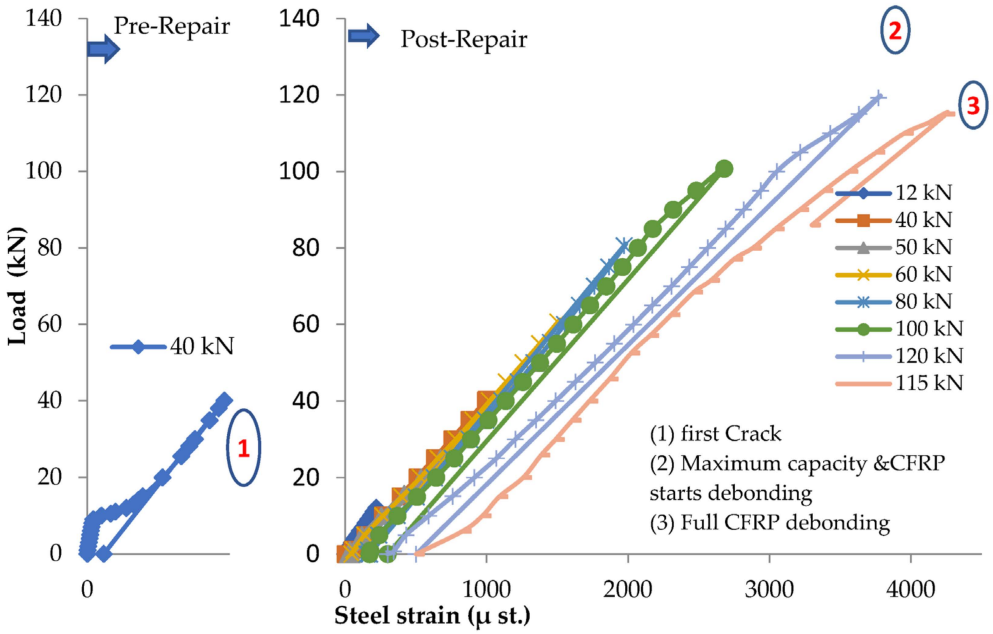

Figure 17. Load against mid-span steel strain curves at pre and post repair stages for beam B112m.

Table 7. Load cycles and corresponding number of cracks for beam B112m.

Load Cycles (kN)	Number of Cracks	Remark
40	9	Pre-repair stage
12	9	Post-repair stage
40	9	
50	14	
60	15	
80	16	
100	18	
120	18	CFRP starts debonding
115	18	Full CFRP debonding
93.5	18	Failure

The results show that the repaired beam can withstand up to 120 kN as the maximum load capacity. The CFRP debonding starts beyond a load of 100 kN, and more cracks in the adhesive layer appear at a load of 120 kN, which leads to full CFRP debonding at a load of 115 kN. The CFRP strain reaches 5700 μst prior to fully debonding. The load drops from 115 kN to 86 kN when the CFRP is deboned. Following this, the beam is loaded again to ascertain the beam capacity with the CFRP sheets fully deboned, which can be considered as the unrepaired beam capacity, where it fails at load 93.5 kN. The steel reaches a strain of 4250 μst when full CFRP debonding occurs, which is less than the rupture strain at 6500 μst, which can be the reason behind the ability of the beam to withstand loads up to 93.5 kN after full CFRP debonding. The increase in the load capacity due to adding the CFRP sheets is evaluated based on the maximum capacity of repaired section (120 kN) divided by the maximum capacity of the unrepaired section (93.5 kN), which gives an increase of 28.4%.

Beam B113m is subjected to a damaged load of 71 kN, close to the steel yield load at the pre-repair stage. After repair, the beam is subjected to load cycles up to failure, where the load cycles and the corresponding number of cracks are shown in Table 8. The load against deflection curves at pre- and post-repair stages are shown in Figure 18. The load against steel strain curves at pre- and post-repair stages are shown in Figure 19. The load against CFRP strain at post-repair stages are shown in Figure 20.

Table 8. Load cycles and corresponding number of cracks for beam B113m.

Load Cycles (kN)	Number of Cracks	Remark
71	15	Pre-repair stage
12	15	Post-repair stage
40	15	
71	16	
80	16	
100	17	
124.7	20	CFRP deboned
101.5	20	Failure

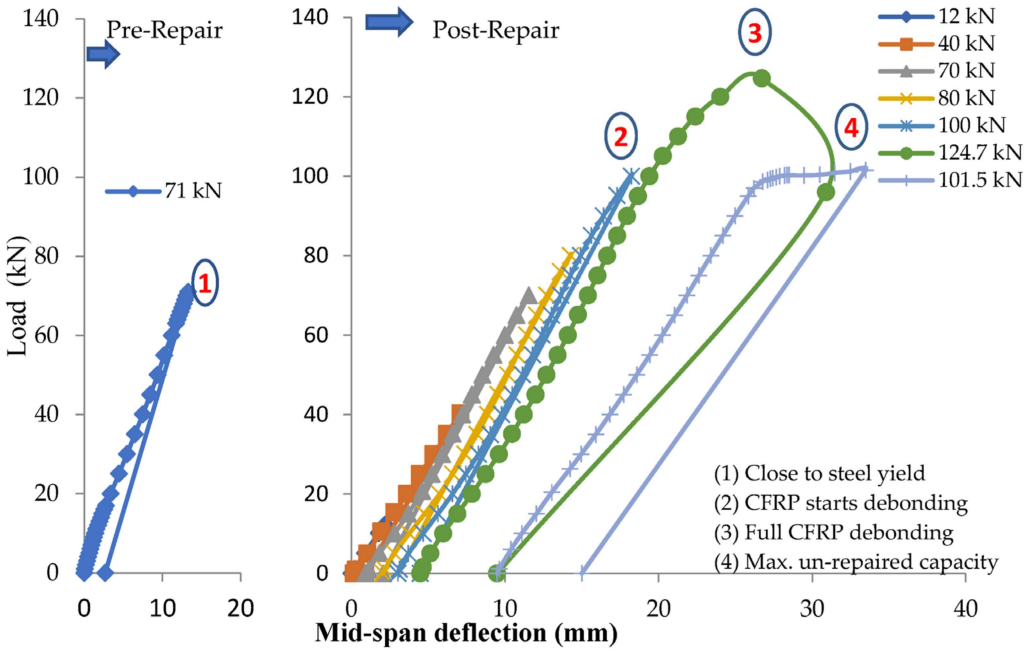

Figure 18. Load against mid-span deflection curves at pre and post repair stages for beam B113m.

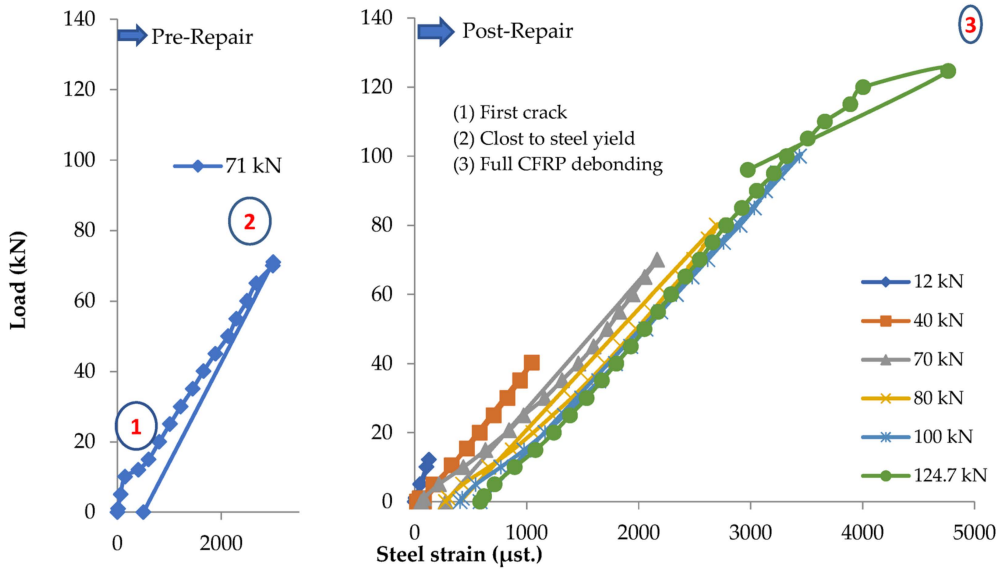

Figure 19. Load against mid-span steel strain curves at pre and post repair stages for beam B113m.

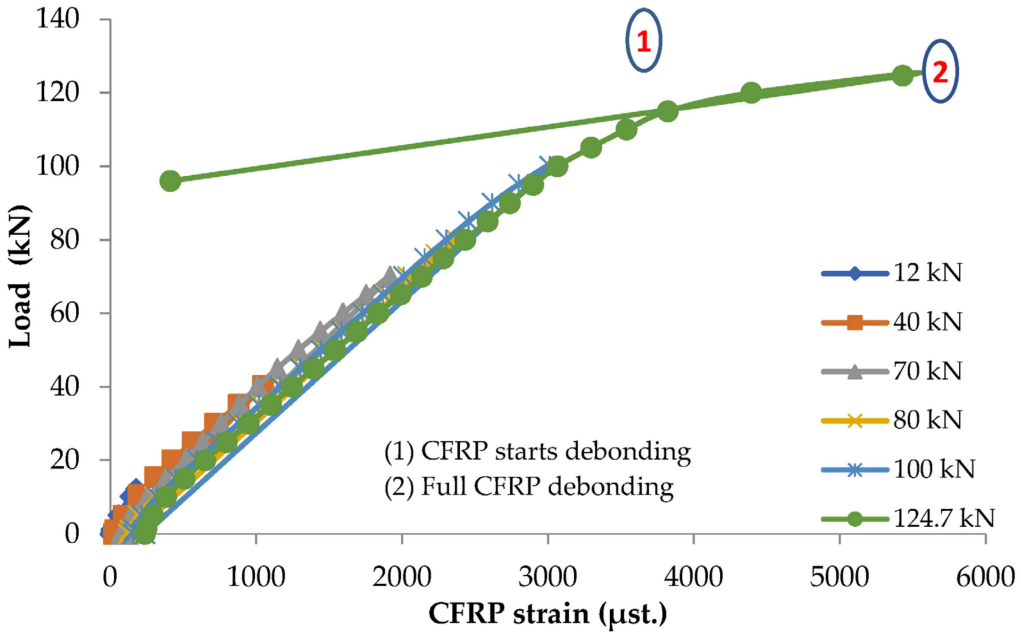

Figure 20. Load against mid-span CFRP strain curves at post-repair stage for beam B113m.

The results show that the beam is damaged under a load of 71 kN, close to the steel yield limit, where the steel reaches a strain of approximately 3000 µst at the pre-repair stage. After repair, the beam can withstand a load of 124.7 kN where full CFRP debonding occurs with a corresponding CFRP strain of 5430 µst. The steel strain reaches 4770 µst when full CFRP debonding occurs, which is less than the rupture limit, and this is the reason behind the ability of the beam to withstand a load of 101.5 kN after full CFRP deboned. The increase in the load capacity by adding the CFRP sheets is evaluated based on the maximum capacity of the repaired section (124.7 kN) divided by the maximum capacity of the unrepaired section (101.5 kN), which gives an increase of 22.8%.

Beam B114m is damaged under the failure load of 82 kN at the pre-repair stage, where the load is applied until the load against the deflection curve becomes horizontal, indicating the start of failure. The steel strain reaches the rupture limit, with a rapid increase in the steel strain beyond the steel yield limit. After repair, the beam is subjected to load cycles up to failure, where the load cycles and the corresponding number of cracks are shown in Table 9. The load against CFRP strain at post-repair stages are as shown in Figure 21. The load against deflection curves at pre- and post-repair stages are shown in Figure 22. The load against steel strain curves at the pre-repair stage are shown in Figure 23, where no data is carried out at the post-repair stages since the train gauge is broken when the failure occurs at the pre-repair stage.

Table 9. Load cycles and corresponding number of cracks for beam B114m.

Load Cycles (kN)	Number of Cracks	Remark
11.5	1	First crack at Pre-repair stage
82	13	Pre-repair stage
40	13	Post-repair stage
70	13	
80	14	
90	14	CFRP starts debonding
93	16	
94.5	16	Full CFRP debonding

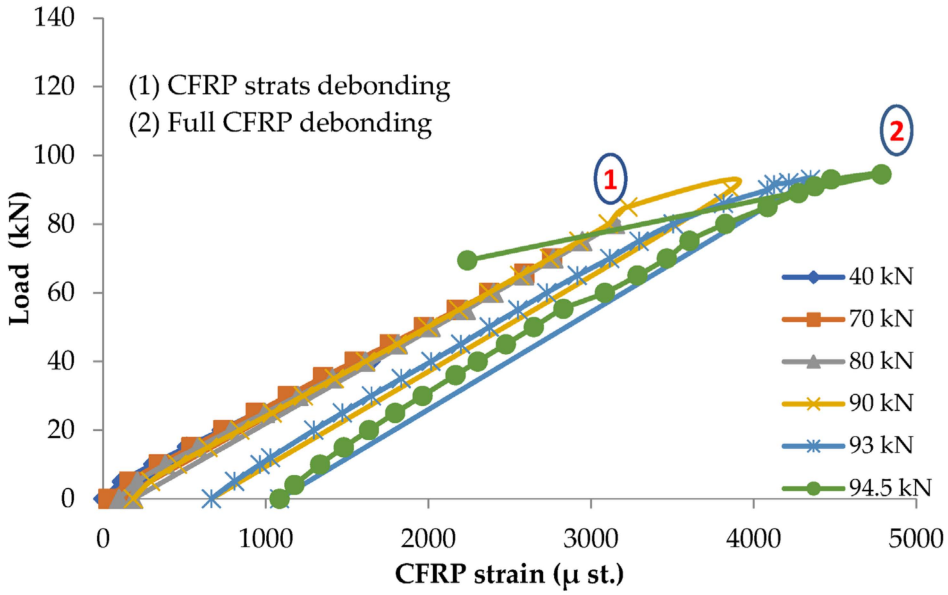

Figure 21. Load against CFRP strain at post-repair stage for beam B114m.

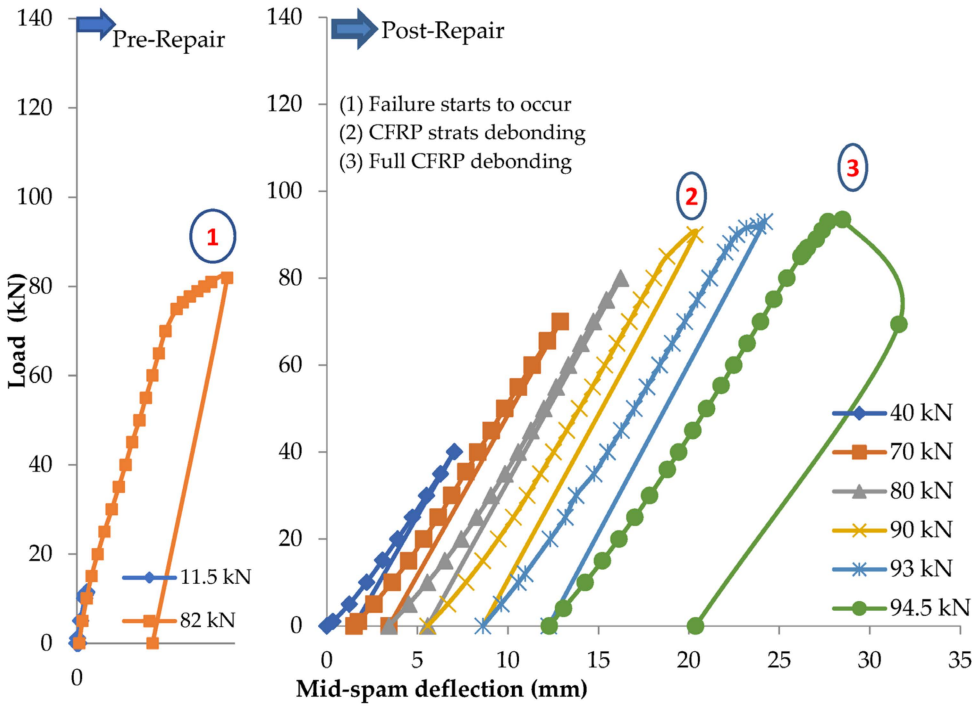

Figure 22. Load against mid-span deflection at pre and post repair stages for beam B114m.

The results show that the beam can withstand loading up to 94.5 kN after repair with externally bonded CFRP sheets. The CFRP starts to deboned at 90 kN and is fully deboned at 94.5 kN with a corresponding CFRP strain of 4800 μst. The increase in the load capacity for beam B114m due to fixing the CFRP sheet is evaluated based on the maximum capacity of the repaired section (94.5 kN) divided by the maximum capacity of the unrepaired section (82 kN), which gives an increase of 15.3%.

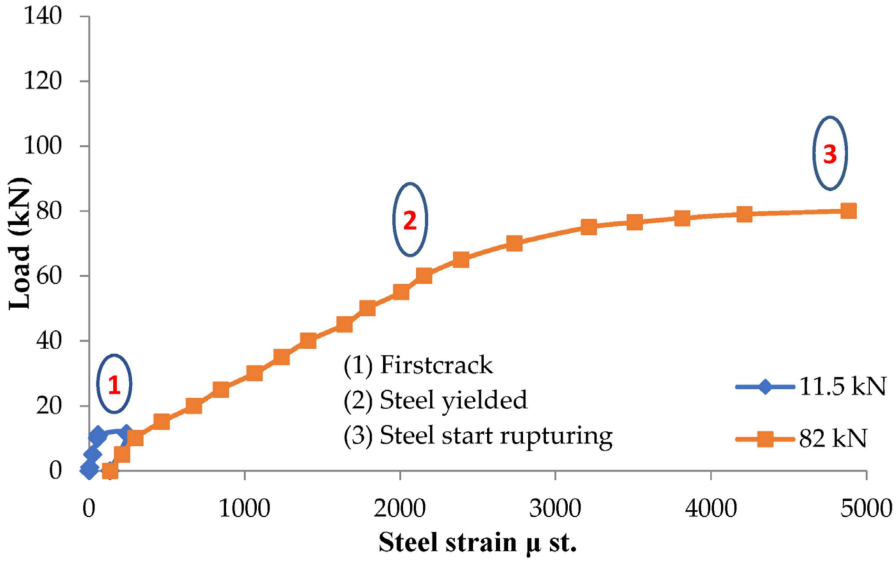

Figure 23. Load against mid-span steel strain at pre-repair stage for beam B114m.

The failure mode is an intermediate-induced crack debonding. The flexural cracks at the mid-span extend to the adhesive interface between the CFRP sheets and the concrete surface, thus inducing intermediate cracks that cause the full CFRP debonding at higher loading. Figure 24 shows the actual cracks in the beam, where intermediate-induced cracks appear in the adhesive layer, and full CFRP debonding occurs. The failure of the CFRP-repaired flexural beams designed with ρmax is governed by the intermediate crack debonding, which is in good agreement with the findings of Büyüköztürk and Hearing [42], and different from the failure observed by Benjeddou et al. [28] which was peeling of CFRP sheets at the ends.

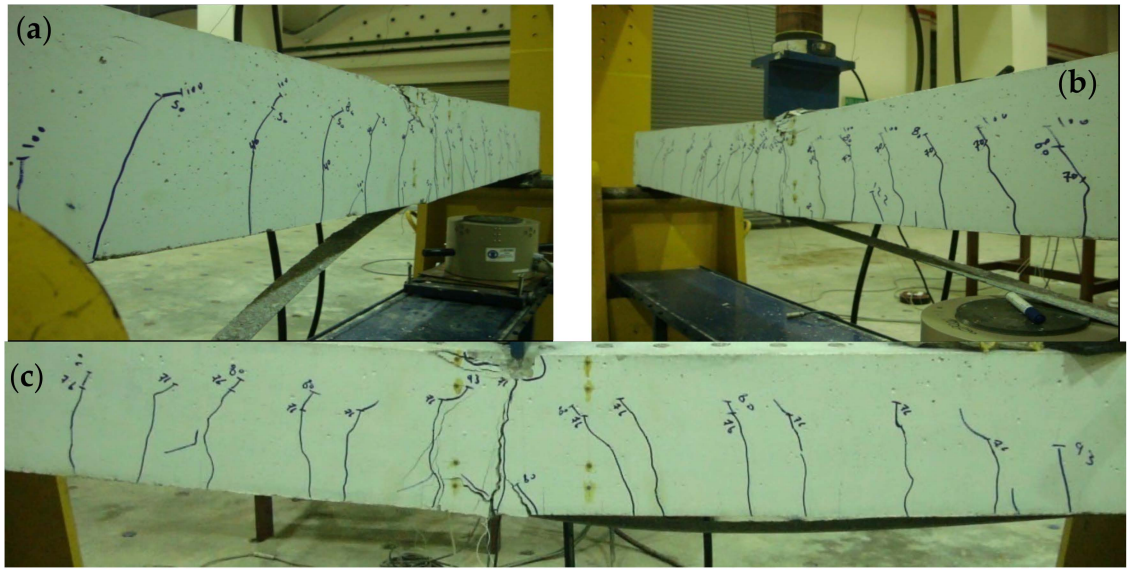

Figure 24. Induced IC debonding and failure mode for beams B112m (**a**), B113m (**b**) and B114m (**c**), from left to right, respectively.

The effectiveness of the CFRP repair system for different pre-repair damage levels and flexural beams designed according to ρmax are presented here. The stiffness recovery based on the static data is calculated based on the ratio of the increased capacity of the repaired sections to the ultimate capacity of the unrepaired sections. Figure 25 shows the repair effectiveness based on the static data and corresponding to the damage levels of beams

B112m, B113m, and B114m. The results show that fixing the CFRP sheets as a flexural repair system for flexural beams with ρmax is effective regardless of the pre-repair damage level. The increase in the load capacity depends on the pre-repair damage level. For a damage level of 43%, close to the design load limit, the repair with CFRP sheets increases the ultimate capacity by 29%. For a pre-repair damage level of 100%, the increase in the load capacity is limited to 15.3%.

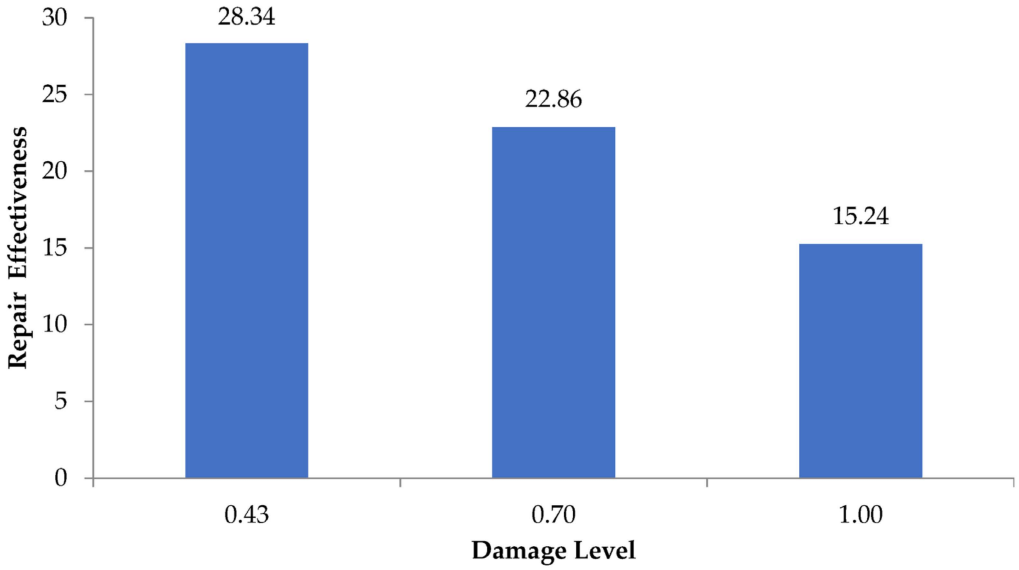

Figure 25. CFRP repair effectiveness based on static data for ρmax group.

3.3. Effect of Steel Ratio

This section summarises the influence of the design criteria concerning the design steel ratio on the effectiveness of the CFRP repair system. It highlights the effect of the steel ratio on the load capacity increase and the failure mode. The provided ρmin is 0.006, and ρmax is 0.0131, where ρmin and ρmax according to the ACI 318 [39] design code, are 0.003 and 0.0136, respectively. According to the ACI 440.2R [40] design code, the beams with the minimum steel ratio are repaired using 100 mm width of the CFRP sheets, while the beams with the maximum steel ratio are repaired using 50 mm width CFRP sheets. The minimum steel group beams increase the capacity of the repair with CFRP sheets to withstand higher load capacity than the maximum steel group. When the pre-repair damage load equals the design load, the increase in load capacity for minimum and maximum steel group beams is 84.5% and 28.3%, respectively. The big difference between the used ρmin, that is, 0.006, and the balanced steel ratio of 0.0182 according to the ACI 318 [39] design code gives the repaired beams the ability to increase the load capacity by 49 to 84.5%. On the other hand, the slight difference between the used ρmax, that is, 0.0131, and the balanced steel ratio, 0.0182, is that the repaired beams have less ability to increase in the load capacity where a limited increase of 15.3 to 28.4% is observed. The load capacity increases for both ρmin and ρmax group beams.

The effect of the pre-repair damage levels on the load capacity increase is affected by the design requirements of the steel ratio. The effect of the pre-repair damage level, which equals the steel yield load, on the increase in the load capacity for ρmin beams, is higher when compared to the ρmax beams. The effects of pre-repair damage level, which equals the failure load, on the increase in the load capacity, is higher for the maximum steel beams. Thus, the repair effectiveness of the RC beams depends on the ratio of the steel provided to the balanced steel.

Flexural cracks at the pre-repair damage stage for both steel ratios govern the failure mode. It is due to intermediate-induced crack debonding, where the flexural cracks

influence the adhesive layer and induce intermediate cracks. The cracks propagate to cause debonding at higher load levels.

4. Conclusions

The following conclusions can be drawn based on the experimental tests and results of this study on CFRP-repaired RC beams in flexural.

- Beams that have a minimal steel limit (min) have been found to have an increased load capacity from 49% to 85%, which corresponds to the pre-repair damage level (design load to failure load). In comparison, the increase in the load capacity for beams with maximum steel limit (max) ranged from 15.3% to 28.4% (design load to failure load); thus, the design steel limit had a considerable influence on the increase in the capacity of the repaired ultimate section.
- The higher the amount of damage that existed before the repair, the lower the efficacy of the repair that was performed utilising CFRP sheets.
- Repair using CFRP sheets helps to enhance the load capacity, which is true regardless of the amount of damage present before the repair, as well as at the level of failure.
- Existing pre-repair flexural fractures at the mid-span extend to the adhesive interface between the CFRP sheets and the concrete surface. As a result, intermediate cracks are induced, which lead to the complete debonding of the CFRP when the loading is increased.
- After the CFRP sheets have been debonded, the beams can still sustain loads near their unrepaired capacity. This demonstrates that it is possible to re-repair the beams despite the debonding of the CFRP sheets.

Author Contributions: Conceptualization, M.M.F. and H.A.R.; Methodology, M.M.F.; Validation, H.A.R.; Formal analysis, M.M.F.; Investigation, M.M.F.; Writing—original draft, M.M.F.; Writing—review & editing, M.M.F.; Visualization, M.M.F.; Supervision, H.A.R.; Funding acquisition, H.A.R. All authors have read and agreed to the published version of the manuscript.

Funding: This research was funded by University of Malaya under Postgrad Fund Program.

Institutional Review Board Statement: Not applicable.

Informed Consent Statement: Not applicable.

Data Availability Statement: Not applicable.

Acknowledgments: The authors would like to acknowledge the financial assistance the University of Malaya provided. The authors would also like to thank all the people who have contributed in any way to making this research possible.

Conflicts of Interest: The authors declare no conflict of interest.

Nomenclature

RC	Reinforced Concrete
FRP	Fibre Reinforced Polymer
CFRP	Carbon Fibre Reinforced Polymer
IC	intermediate-induced crack
ACI	American Concrete Institute
GFRP	Glass Fibre Reinforced Polymer
ρmax	maximum steel limit
ρmin	minimum steel limit

References

1. Bakis, C.E.; Bank, L.C.; Cosenza, E.; Davalos, J.F.; Lesko, J.J.; Machida, A.; Rizkalla, S.H.; Triantafillou, T. Fiber-reinforced polymer composites for construction—State-of-the-art review. *J. Compos. Constr.—ASCE* **2002**, *6*, 73–87. [CrossRef]
2. Teng, J.G.; Chen, J.F.; Smith, S.T.; Lam, L. *FRP-Strengthened RC Structures*; John Wiley & Sons Ltd.: Chichester, UK, 2001.

3. Almakt, M.M.; Balazs, G.L.; Pilakoutas, K. Strengthening of RC Elements by CFRP Plates Local Failure. In Proceedings of the 2nd International PhD Symposium in Civil Engineering, Budapest, Hungary, 28–30 May 1999.
4. Fanning, P.J.; Kelly, O. Ultimate response of RC beams strengthened with CFRP plates. *J. Compos. Constr.—ASCE* **2011**, *5*, 122–127. [CrossRef]
5. Nguyen, D.M.; Chan, T.K.; Cheong, H. brittle failure and bond development length of CFRP-concrete beams. *J. Compos. Constr—ASCE* **2001**, *5*, 12–17. [CrossRef]
6. Barros, J.A.O.; Ferreira, D.R.S.M.; Fortes, A.S.; Dias, S.J.E. Assessing the effectiveness of embedding CFRP laminates in the near surface for structural strengthening. *Constr. Build. Mater.* **2006**, *20*, 478–491. [CrossRef]
7. Ghosh, K.K.; Karbhari, V.M. Evaluation of strengthening through laboratory testing of FRP rehabilitated bridge decks after in-service loading. *Compos. Struct.* **2007**, *77*, 206–222. [CrossRef]
8. Decker, B.R. A Method of Strengthening Monitored Deficient Bridges. Master's Thesis, Kansas State University, Manhattan, KS, USA, 2007.
9. Jeevan, N.; Reddy, H.N.J. Strengthening of RC beams using externally bonded laminate (EBL) technique with end anchorages under flexure. *Asian J. Civ. Eng.* **2018**, *19*, 263–272. [CrossRef]
10. Al-Khafaji, A.; Salim, H. Flexural Strengthening of RC Continuous T-Beams Using CFRP. *Fibers* **2020**, *8*, 41. [CrossRef]
11. White, T.W.; Soudki, K.A.; Erki, M.A. Response of RC beams strengthened with CFRP laminates and subjected to a high rate of loading. *J. Compos. Constr.—ASCE* **2001**, *5*, 153–162. [CrossRef]
12. Capozucca, R.; Cerri, M.N. Static and dynamic behaviour of RC beam model strengthened by CFRP-sheets. *Constr. Build. Mater.* **2002**, *16*, 91–99. [CrossRef]
13. Jumaat, M.Z.; Ashraful-Alam, M.D. Problems associated with plate bonding methods of strengthening reinforced concrete beams. *J. Appl. Sci. Res.* **2006**, *2*, 703–708.
14. Choo, C.C.; Zhao, T.; Harik, I. Flexural retrofit of a bridge subjected to overweight trucks using CFRP laminates. *Compos. Part B Eng.* **2007**, *38*, 732–738. [CrossRef]
15. Al-Saidy, A.H.; Al-Harthy, A.S.; Al-Jabri, K.S.; Abdul-Halim, M.; Al-Shidi, N.M. Structural performance of corroded RC beams repaired with CFRP sheets. *Compos. Struct.* **2010**, *92*, 1931–1938. [CrossRef]
16. El-Ghandour, A.A. Experimental and analytical investigation of CFRP flexural and shear strengthening efficiencies of RC beams. *Constr. Build. Mater.* **2011**, *25*, 1419–1429. [CrossRef]
17. Cromwell, J.R.; Harries, K.A.; Shahrooz, B.M. Environmental durability of externally bonded FRP materials intended for repair of concrete structures. *Constr. Build. Mater.* **2011**, *25*, 2528–2539. [CrossRef]
18. Fayyadh, M.M.; Abdul Razak, H. Assessment of effectiveness of CFRP repaired RC beams under different damage levels based on flexural stiffness. *Constr. Build. Mater.* **2012**, *37*, 125–134. [CrossRef]
19. Fayyadh, M.M.; Abdul Razak, H. Analytical and experimental study on repair effectiveness of CFRP sheets for RC beams. *J. Civ. Eng. Manag.* **2014**, *20*, 21–31. [CrossRef]
20. Hosen, M.A.; Jummat, M.Z.; Alengaram, U.J.; Sulong, N.H.R.; Saiful-Islam, A.B.M. Structural performance of lightweight concrete beams strengthened with side-externally bonded reinforcement (S-EBR) technique using CFRP fabrics. *Compos. Part B Eng.* **2019**, *176*, 107323. [CrossRef]
21. Vuković, N.K.; Jevrić, M.; Zejak, R. Experimental Analysis of RC Elements Strengthened with CFRP Strips. *Mech. Compos. Mater.* **2020**, *56*, 75–84. [CrossRef]
22. Jeevan, N.; Reddy, H.N.J.; Prabhakara, R. Flexural strengthening of RC beams with externally bonded (EB) techniques using prestressed and non-prestressed CFRP laminate. *Asian J. Civ. Eng.* **2019**, *19*, 893–912. [CrossRef]
23. Ahmed, A.; Naganathan, S.; Nasharuddin, K.; Fayyadh, M.M.; Hamali, S. Repair Effectiveness of Damaged RC Beams with Web Opening Using CFRP and Steel Plates. *Jordan J. Civ. Eng.* **2016**, *10*, 163–183.
24. Xie, H.B.; Wang, Y.F. Reliability Analysis of CFRP-Strengthened RC Bridges Considering Size Effect of CFRP. *Materials* **2019**, *12*, 2247. [CrossRef] [PubMed]
25. Fayyadh, M.M.; Abdul Razak, H. The effect of CFRP-concrete bond mechanism on dynamic parameters of repaired concrete girders. *Struct. Eng. Mech.* **2022**, *82*, 343–354. [CrossRef]
26. Fayyadh, M.M. Modified models to predict the ultimate flexural and shear capacities of CFRP repaired RC beams. *Adv. Comput. Design* **2021**, *6*, 99–115. [CrossRef]
27. Ross, C.A.; Jerome, D.M.; Tedesco, J.W.; Hughes, M.L. Strengthening of reinforced concrete beams with externally bonded composite laminates. *ACI Struct. J.* **1999**, *96*, 212–220.
28. Benjeddou, O.; Ouezdou, M.B.; Bedday, A. Damaged RC beams repaired by bonding of CFRP laminates. *Constr. Build. Mater.* **2007**, *21*, 1301–1310. [CrossRef]
29. Fam, A.; MacDougall, C.; Shaat, A. Upgrading steel–concrete composite girders and repair of damaged steel beams using bonded CFRP laminates. *Thin-Wall. Struct.* **2009**, *47*, 1122–1135. [CrossRef]
30. Kim, Y.J.; Brunell, G. Interaction between CFRP-repair and initial damage of wide-flange steel beams subjected to flexure. *Compos. Struct.* **2011**, *93*, 1986–1996. [CrossRef]
31. Erki, M.A.; Meier, U. Impact loading of concrete beams externally strengthened with CFRP laminates. *J. Compos. Constr.—ASCE* **1999**, *3*, 117–124. [CrossRef]

32. Rahimi, H.; Hutchinson, A. Concrete beams strengthened with externally bonded FRP plates. *J. Compos. Constr.—ASCE* **2001**, *5*, 44–56. [CrossRef]
33. Badawi, M.; Soudki, K. Flexural strengthening of RC beams with prestressed NSM CFRP rods—Experimental and analytical investigation. *Constr. Build. Mater.* **2009**, *23*, 3292–3300. [CrossRef]
34. Nassiraei, H.; Rezadoost, P. Static capacity of tubular X-joints reinforced with fiber reinforced polymer subjected to compressive load. *Eng. Struct.* **2021**, *236*, 112042. [CrossRef]
35. Fayyadh, M.F.; Abed, M.J. Utilizing CFRP and steel plates for repair of damaged RC beams with circular web openings. *Struct. Eng. Mech.* **2022**, *84*, 49–61. [CrossRef]
36. Fayyadh, M.F.; Abdul-Razak, H. Impact of design parameters and cycles of damage loads on CFRP repair effectiveness of Shear-Deficient RC structures. *Constr. Build. Mater.* **2022**, *347*, 128465. [CrossRef]
37. Hawileh, R.A.; Nawaz, W.; Abdalla, J.A.; Saqan, E.I. Effect of flexural CFRP sheets on shear resistance of reinforced concrete beams. *Compos. Struct.* **2014**, *122*, 468–476. [CrossRef]
38. Elkhabeery, O.H.; Safar, S.S.; Mourad, S.A. Flexural strength of steel I-beams reinforced with CFRP sheets at tension flange. *J. Constr. Steel Res.* **2018**, *148*, 572–588. [CrossRef]
39. *ACI 318*; Building Code Requirements for Structural Concrete and Commentary. American Concrete Institute: Farmington Hills, MI, USA, 2008.
40. *ACI 440.2R*; Guide for the Design and Construction of Externally Bonded FRP Systems for Strengthening Concrete Structures. American Concrete Institute: Farmington Hills, MI, USA, 2002.
41. Fayyadh, M.M.; Abdul Razak, H. Assessment of adhesive setting time in reinforced concrete beams strengthened with carbon fibre reinforced polymer laminates. *Mater. Des.* **2012**, *37*, 64–72. [CrossRef]
42. Büyüköztürk, O.; Hearing, B. Failure behavior of precracked concrete beams retrofitted with FRP. *J. Compos. Constr.—ASCE* **1998**, *2*, 138–144. [CrossRef]